Gary Drzewiecki, Shawn Field, Issam Moubarak and John K.-J. Li

You might find this additional information useful...

This article cites 18 articles, 5 of which you can access free at:
http://ajpheart.physiology.org/cgi/content/full/273/4/H2030#BIBL

Medline items on this article's topics can be found at http://highwire.stanford.edu/lists/artbytopic.dtl
on the following topics:
Medicine .. Femoral Artery
Physiology .. Jugular Veins
Physiology .. Blood Pressure
Medicine .. Etiology

Updated information and services including high-resolution figures, can be found at:
http://ajpheart.physiology.org/cgi/content/full/273/4/H2030

Additional material and information about *AJP - Heart and Circulatory Physiology* can be found at:
http://www.the-aps.org/publications/ajpheart

This information is current as of September 14, 2007 .

modeling in physiology

Vessel growth and collapsible pressure-area relationship

GARY DRZEWIECKI, SHAWN FIELD, ISSAM MOUBARAK, AND JOHN K.-J. LI
Cardiovascular Research Laboratory, Department of Biomedical Engineering, Rutgers,
The State University of New Jersey, Piscataway, New Jersey 08855-0909

Drzewiecki, Gary, Shawn Field, Issam Moubarak, and John K.-J. Li. Vessel growth and collapsible pressure-area relationship. *Am. J. Physiol.* 273 (*Heart Circ. Physiol.* 42): H2030–H2043, 1997.—The role that the pattern of vessel wall growth plays in determining pressure-lumen area (P-A) and pressure-compliance curves was examined. A P-A vessel model was developed that encompasses the complete range of pressure, including negative values, and accounts for size given the fixed length, nonlinear elastic wall properties, constant wall area, and collapse. Data were obtained from excised canine carotid and femoral arteries, jugular veins, and elastic tubing. The mean error of estimate was 8 mmHg for all vessels studied and 2 mmHg for blood vessels. The P-A model was employed to examine two patterns of arterial wall thickening, outward growth and remodeling (constant wall area), under the assumption of constant wall properties. The model predicted that only outward wall growth resets compliance such that it increases at a given arterial pressure, explaining previously contradictory data. In addition, it was found that outward wall growth increases the lumen area between normal and high pressures. Remodeling resulted in lumen narrowing and a decrease in compliance for positive pressures.

vascular pressure-area model; arterial hypertrophy; arterial remodeling; hypertension

ARTERIAL WALL HYPERTROPHY is a process associated with systemic hypertension. The pressure-area (P-A) curve of the vessel reflects this alteration and is important in determining the hemodynamic response. In early hypertension, vascular wall thickening appears to be an adaptive mechanism that responds to increases in the vessel wall tension (21). A recent study (17) examined the growth patterns of arteries during hypertension. For example, it has been found that the vessel wall grows such that the wall thickness increases and the lumen area narrows. The classic observation is that the wall thickness-to-diameter ratio is increased, perhaps in accordance with Laplace's law such that wall stress is maintained (12). In this case, the growth may occur either through hypertrophy, where the cells increase their size, or through hyperplasia by cell division and through deposits to the connective tissue matrix (28). Alternatively, vascular remodeling may occur where it is defined that the wall cross-sectional area remains constant while wall thickening takes place (17). To have complete remodeling, the vessel diameter must decrease with increases in wall thickness. In this situation, there is no growth but rearrangement of wall material. Thus a constant wall cross-sectional area defines whether wall thickening is due to remodeling. Studies have shown that small arteries remodel during hypertension. If growth is present, it is typically due to hyperplasia (17).

Because wall thickness increases with hypertension, it is generally believed that vascular compliance and lumen area decrease. Recent data on large arteries apparently contradict this notion (1, 16), where it has been found that both lumen area and compliance increase in hypertensive subjects. It is difficult to explain this discrepancy because the wall properties of hypertensive vessels tend to increase in stiffness and smooth muscle activation (5), leading to the opposite conclusion. It is hypothesized here that the pattern of wall thickening may explain this observation and, in general, that vessel structure has a major influence on the distension properties of arteries.

In this paper, the effect of vascular growth pattern on the relationship between pressure, lumen area, and compliance is examined by means of a mathematical model. The model is developed in this paper and is useful in providing the P-A curve of vessels for application to hemodynamic studies. The model is also validated with data obtained from excised artery, vein, and elastic vessel experiments. The data are used to establish the normal values of vessel wall properties and geometry that are expressed as the parameters of the model. In this manner, the arterial function can be analyzed with respect to its structure (23). Then, with these parameters as the control values, two patterns of wall thickening are studied: remodeling and outward wall thickening. This is accomplished by varying only the size parameters of the model to reflect these patterns of growth and computing the P-A curve of the hypertrophied vessel while wall properties are maintained.

Glossary

a	Constant of proportionality termed elastance scale modulus
a'	Constant of proportionality termed wall elastic scale modulus
a_1	Linear elastance constant
a_2	Quadratic elastance constant
a_1'	Linear wall elasticity constant
a_2'	Quadratic wall elasticity constant
b	Exponential rate constant termed elastance rate modulus

b'	Exponential rate constant termed wall elastic rate modulus
c	Hyperbolic rate constant for stretch equation
h	Vessel wall thickness
h_b	Vessel wall thickness at MCP
h_{bc}	Control value of vessel wall thickness for normal nonhypertrophied artery at MCP
n	Constant defining degree of curvature of pressure-area hyperbola
r	Vessel lumen radius
r_b	Vessel lumen radius at MCP
r_{bc}	Control value of vessel lumen radius for normal nonhypertrophied artery at MCP
r_m	Midwall vessel lumen radius
r_{mb}	Midwall vessel lumen radius at MCP
r_0	Vessel lumen radius when wall tangential stress is zero; i.e., when $P_t = 0$
A	Lumen cross-sectional area
A_b	Lumen cross-sectional area at MCP
A_0	Lumen cross-sectional area when $P_t = 0$
A_w	Vessel wall cross-sectional area
C_a	Area compliance of vessel segment
C_V	Volume compliance of vessel segment
C_{max}	Maximum compliance
E	Wall elastic modulus (elasticity)
E_c	Area elastance of vessel segment
EI	Constant of proportionality termed flexural rigidity
$\widehat{EI}$	Flexural rigidity normalized by lumen radius cubed
L	Vessel segment length
MCP	Maximum compliance point
P-A	Transmural pressure-area relationship
P_b	Buckling pressure (transmural pressure at MCP)
P_c	Pressure due to vessel bending (collapse)
P_s	Pressure due to vessel mean wall stress
P_t	Transmural pressure; pressure across the vessel wall
V	Lumen volume of vessel segment
γ	Ratio defined as h_{bc}/r_{bc}
λ	Vessel wall tangential extension ratio
λ_m	Vessel wall tangential extension ratio at midwall
λ_s	Wall extension ratio for stretch only
λ_{sm}	Wall extension ratio at midwall for stretch only
$\overline{\sigma}$	Mean vessel wall tangential stress

BACKGROUND

The volume compliance of a vessel is one of the three primary physical parameters of a vascular dynamic system, the others being flow inertance and fluid resistance. Compliance is defined as the derivative of volume (or cross-sectional area) of a vessel with respect to the fluid pressure across the vessel wall (i.e., transmural pressure), or mathematically

$$C_V = \frac{dA}{dP_t} \times L = \frac{dV}{dP_t} \qquad (1)$$

This equation assumes a uniform pressure and area with length, such that $V = AL$. A typical P-A curve for a blood vessel is nonlinear (Fig. 1*A*). As a result of this, compliance must be evaluated as a function of transmural pressure or lumen area (Fig. 1*B*) (19). Thus it is appropriate to employ a constant arterial compliance only when the change in pressure is small. Constant compliance is often assumed in models of the systemic arterial system (30). The relief of this approximation
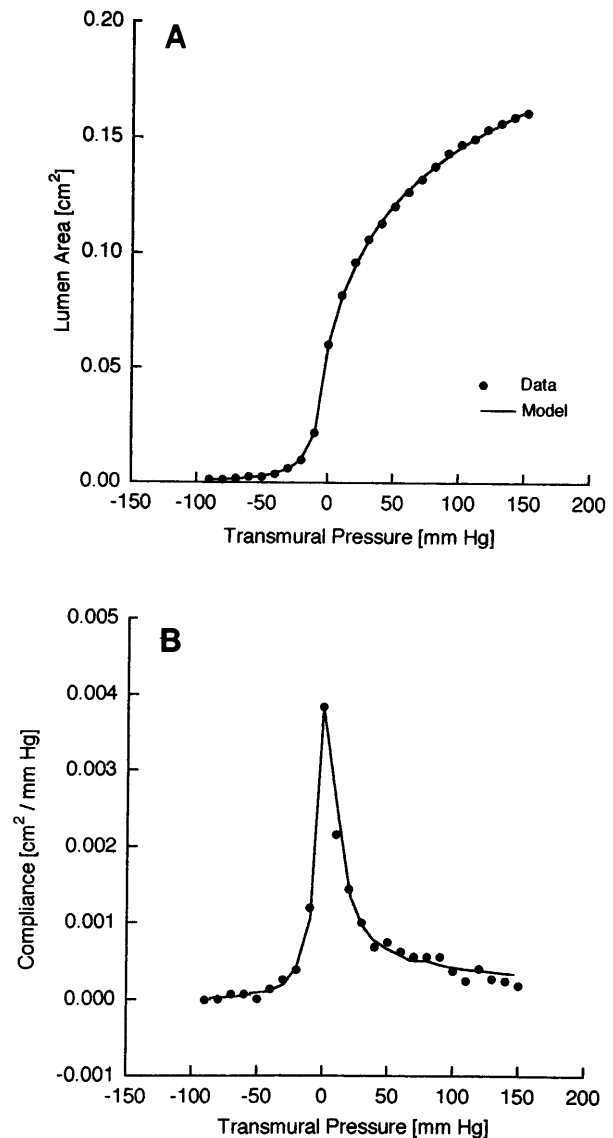

Fig. 1. *A*: pressure-area (P-A) relationship for a canine carotid artery from physical data and model prediction (lumped model; *Eq. 9*). Curve takes on a sigmoidal shape, indicating 2 different regions of mechanical behavior. *B*: corresponding compliance-pressure curve from data and model results in *A* computed with *Eq. 1*.

has been shown to be useful when transmural pressure varies significantly, such as during the generation of Korotkoff sounds (6). The P-A curve approximates a sigmoidal relationship involving two regions of physical behavior. The upper positive-pressure region is due to vessel wall stretch while the vessel lumen is circular. This behavior is the result of nonlinear wall elasticity that can be modeled by an exponential stress-strain relationship (13, 15) of the form

$$\overline{\sigma} = a'(e^{b'\lambda} - 1) \qquad (2)$$

$$\lambda = \frac{r - r_0}{r_0} \qquad (3)$$

λ is defined by the fractional change in lumen radius from its initial value. Wall stress due to distension is

assumed to be zero when $r_0 = r$. Wall stress becomes compressive below this radius and transmural pressure is negative.

Low to negative transmural pressures applied uniformly over a uniform segment of vessel eventually result in collapse or distortion of the originally circular profile (13, 20, 22). This occurs due to buckling of the vessel wall. Negative transmural pressure is then supported by vessel wall bending. Thus the P-A relationship follows that of a pressure-loaded elastic cantilever beam and yields a one-branch hyperbolic relationship, as follows (13, 25)

$$P_t = -\frac{EI}{r_b^3}\left[\left(\frac{A_b}{A}\right)^n - 1\right] + P_b \qquad (4)$$

The P-A relationship described by *Eq. 4* is a result of the change in the cross-sectional shape of the vessel lumen, not to wall stretch as in *Eqs. 2* and *3*. The details of this shape have been analyzed previously by others (11, 18, 20). Generally, though, it is not necessary to know the shape for most hemodynamic studies except when the lumen area approaches zero.

Previous mathematical representations of the steady-state arterial P-A relationship involved assumptions that are not justifiable (8). Several of these assumptions are that *1*) the pressure range is positive only, *2*) the volume is zero at zero pressure, *3*) the compliance is zero at zero pressure, *4*) the shape of the P-A curve is a simple exponential (not sigmoidal) or is linear (constant compliance), *5*) the model parameters are often not unique, and *6*) the model parameters cannot be related to measurable vessel mechanics and wall properties.

Furthermore, previous models were designed to serve a limited range of P-A data, thus not permitting extrapolation. These models were also not versatile enough in representing both vascular data from different vessel types and elastic tube data. Last, the models were often empirical formulas that could not be related directly to vessel mechanics. For example, Sipkema and Westerhof (26) assumed a trigonometric tangent function. This function, although a good fit in the collapse region, is in error for high pressure extremes, predicting zero-compliance values. Another example is a finite-order polynomial such as that used by Beyar et al. (3). Applying a polynomial to fit a transcendental curve, such as the P-A curve, will cause extrapolation error. The present model overcomes all of the above drawbacks without making any of the previously stated assumptions. To attest to the versatility of the model, it will be applied to three types of vessel: artery, vein, and latex elastic tubing.

BLOOD VESSEL P-A MODEL

Basic Derivation (Lumped Model)

The vessel model was derived by formulating a unique mathematical description of nonlinear vessel distension and collapse (10). Specifically, *Eqs. 2* and *3* were transformed from a stress-to-extension ratio relationship into a corresponding P-A relationship. This

was accomplished by converting $\overline{\sigma}$ into pressure through a modified Laplace equation for a thin-walled cylinder (13)

$$P_s = \overline{\sigma}\,\frac{h}{r} \qquad (5)$$

The radial extension ratio was converted to area strain by substituting $r = (A/\pi)^{1/2}$ into *Eq. 3*.

To combine the equations for vessel distension and collapse regions, the extension ratio was redefined in terms of A/A_b instead of A/A_0. It was chosen to reference strain to the onset of buckling because this point is easily identified on the P-A curve. Also, buckling can be easily located on a graph of compliance-area or compliance-pressure as the MCP by definition. Thus the lumen area at which buckling occurs arises at a transmural pressure of P_b. Although the P_b can be predicted theoretically from the buckling criteria of von Mises (27), it was chosen instead to locate P_b directly from vessel data. Thus the distension equation was solved for the P_b by substituting $A = A_b$ to yield

$$P_s = a[e^{b(A_b/A_0-1)} - 1] = P_b \qquad (6)$$

Because the buckling area is normally less than the zero-pressure area, *Eq. 6* reveals that the P_b is negative in value. The distension pressure equation can then be modified by substituting A_b for A_0 and adding P_b as follows

$$P_s = a[e^{b(A/A_b-1)} - 1] + P_b \qquad \text{for } A > A_b \qquad (7a)$$

and

$$P_s = P_b \qquad\qquad \text{for } A = A_b$$
$$\tag{7b}$$

Thus for *Eq. 7* to be true requires that A_b be substituted for A_0. The inequality denotes the transition between buckling and wall stretch. Once buckling occurs, the perimeter of the vessel remains unchanged. *Equation 7a* can be modified to incorporate this concept by limiting the vessel perimeter to one corresponding with that of A_b for values of $A < A_b$. This can be accomplished by introducing a hyperbolic relationship into *Eq. 7a* as follows

$$P_s = a(e^{b\lambda_s} - 1) + P_b \qquad (8a)$$

where the extension ratio is

$$\lambda_s = [1 + (A/A_b)^c]^{1/c} - 1 \qquad (8b)$$

Normally, the value of c is not critical but was chosen as $c > 20$ such that λ_s is forced to zero quickly when $A < A_b$. In this case, wall stretch has no effect below the buckling area and pressure depends only on the buckling stresses. The modified forms of *Eqs. 4* and *8* were then combined into the entire P-A relationship

$$P_t = a[e^{b(A-A_b)/A_b} - 1] - \widehat{EI}\left[\left(\frac{A_b}{A}\right)^n - 1\right] + P_b \qquad (9)$$

where $\widehat{EI}$ was substituted for EI/r^3. At any given lumen area, the terms of *Eq. 9* represent the summation of pressures due to vessel wall stretch, bending (collapse),

and buckling ($P_s + P_c + P_b = P_t$), respectively. This is shown in Fig. 2, where the pressure due to stretch and the pressure due to buckling and collapse are separated. The total pressure is also shown as the summation for what would be similar to a linear elastic vessel. Note, also, that the pressure due to distension was zero below the buckling pressure but that the pressure due to collapse was permitted to have a value into the range of distension. During this range of pressure, the vessel was allowed to bend and stretch simultaneously (20). Bending stresses stabilize at high pressures where the vessel lumen becomes circular in shape.

The compliance equation can be derived by taking the inverse of the derivative of *Eq. 9* as stated previously. The equation for the E_c is

$$\frac{dP_t}{dA} = E_c = \frac{1}{C_a} = \frac{ab}{A_b}e^{b\lambda} + \widehat{EI}nA_b^n\left(\frac{1}{A}\right)^{n+1} \qquad (10)$$

Approximate form. It was found useful to approximate the exponential stretch relationship in *Eq. 9* of the model. The first two terms of a Taylor series were employed, consisting of the first and second power of the extension ratio. In this case, the model equation becomes

$$P_t = a_1\lambda + a_2\lambda^2 - \widehat{EI}\left[\left(\frac{A_b}{A}\right)^n - 1\right] + P_b \qquad (11)$$

It was found that the advantage of this formulation is that it can represent both linear elastic vessels and blood vessels equally well. For example, if the vessel is
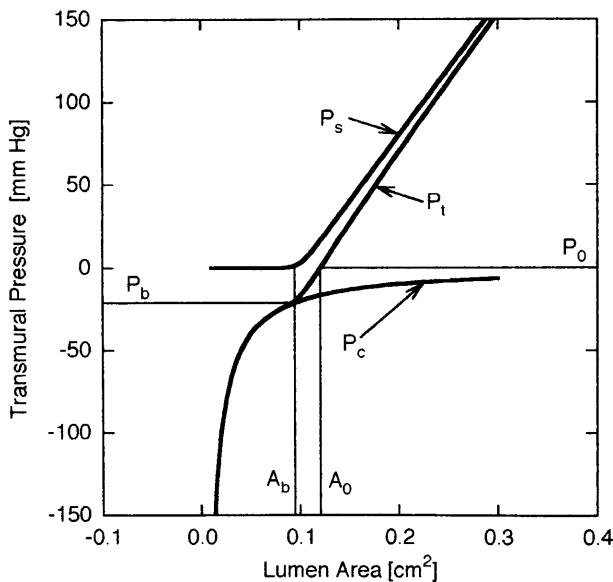

Fig. 2. Model collapse and distension pressures. P_t, transmural pressure-lumen area curve for a hypothetical elastic vessel; P_s, pressure-lumen area curve due to wall stretch alone; P_c, pressure-lumen area curve due to change in cross-sectional geometry and collapse; P_b, buckling pressure (transmural pressure at maximum compliance point); P_0, zero pressure; A_b, lumen cross-sectional area at maximum compliance point; A_0, lumen cross-sectional area at zero transmural pressure. All curves were computed from their corresponding terms in model (*Eq. 9*). P_0-A_0 point is lumen area at which pressure is zero. P_b-A_b is point of onset of buckling.

linear elastic, then the value of a_2 would be zero. Although the exponential relationship can be forced to behave in a nearly linear manner by reducing the value of *b*, it cannot fit a linear elastic vessel as well as *Eq. 11*. There was found to be no statistical disadvantage in using *Eq. 11* compared with *Eq. 9* for nonlinear elastic blood vessels. Moreover, the number of parameters is the same so that nonlinear regression algorithms were found to perform identically for both models.

Geometric P-A Model

The model parameters in *Eq. 9* or *11* can be derived from geometric and wall property vessel data, a first-principle formula, or a statistical fit of the model to vessel P-A data. These parameters indirectly reflect vessel size and wall properties. An alternative model was derived to relate vessel wall thickness, radius, and wall properties directly to the P-A model. Moreover, because the walls of arteries and veins are mostly water, they are nearly incompressible. It was assumed, then, that the wall cross-sectional area is approximately conserved. This assumption was also applied to elastic tubing.

To begin, an equation for wall thickness and radius was derived by equating the wall cross-sectional area at the MCP with the wall cross-sectional area at any other point, relying on conservation of wall cross-sectional area. A second-order polynomial with respect to wall thickness resulted and was solved for wall thickness, obtaining the following equation

$$h = [r^2 + 2(r_b \cdot h_b) + h_b^2]^{1/2} - r \qquad (12)$$

The lumen radius was derived from the lumen area by assuming a circular cross-sectional shape. This assumption holds for pressures at and above the buckling pressure. For pressures less than P_b, $r = r_b$ and $h = h_b$ because the midwall perimeter is constant. At the MCP, the cross-sectional shape may deviate from circular, depending on the vessel. For example, the shape may be more accurately described as elliptical; thus r_b is estimated from the equivalent area of a circle when $A = A_b$. When the vessel collapses, the use of a single value for the radius is meaningless, whereas the use of lumen area still applies.

The mean circumferential wall stress due to stretch was defined by *Eq. 2* modified as

$$\overline{\sigma} = a'(e^{b'\lambda_m} - 1) \qquad (13)$$

where

$$r_m = r + \frac{h}{2} \qquad (14)$$

and where the extension ratio is

$$\lambda_m = \frac{r_m - r_{mb}}{r_{mb}} \qquad (15)$$

The constant r_{mb} is the midwall radius at the MCP when $h = h_b$ and $r = r_b$. A prime denotes wall elastic material property as opposed to unprimed parameters

that were used earlier to indicate an elastance property. As in the lumped model, it is useful to limit the extension ratio to positive values. The extension ratio then becomes

$$\lambda_m = [1 + (r_m/r_{mb})^c]^{1/c} - 1 \qquad (16)$$

Similarly, a series approximation for exponential wall stress can be employed as before. In this case, the mean wall tangential stress becomes

$$\overline{\sigma} = a_1'\lambda_m + a_2'\lambda_m^2 \qquad (17)$$

The stress-strain *Eq. 13* or *17* can be differentiated to obtain the incremental elastic modulus of the wall material. Because the value of b' is positive for blood vessels, the elastic modulus increases with vessel distension; that is, wall stiffness increases. The pressure due to wall stretch was derived through a modified form of the Laplace equation for a thick-walled cylinder

$$P_s = \overline{\sigma}\frac{h}{r_m} \qquad (18)$$

The region of collapse was modeled predominantly by *Eq. 4* where geometric constants and wall elasticity are substituted for the flexural rigidity (13)

$$P_c = -\frac{Eh_b^3}{9r_{mb}^3}\left[\left|\frac{A_b}{A}\right|^n - 1\right] \qquad (19)$$

Note that the flexural or bending properties were referenced to the MCP (A_b, P_b, and C_{max}), where h_b, r_{mb}, and E are assumed to be constant during collapse because there is little wall stretch. Then, as before, the sum of P_s, P_c, and P_b derived in this section is the P_t; that is

$$P_t = P_s + P_c + P_b \qquad (20)$$

VESSEL EXPERIMENTS

Data Collection

P-A data were collected for a total of six vessels: Penrose drainage latex tubing (0.25 in. ID; Davol), Kent latex tubing (0.1875 in. ID), Tygon latex tubing (0.135 in. ID), canine femoral artery, canine carotid artery, and canine jugular vein. Six trials were performed for each vessel. Note that the vessels of interest are medium sized because these vessels have some influence on systemic pressure-compliance and pressure-volume relationships. Alternatively, small peripheral arteries exert their influence on the peripheral flow resistance property (not studied here). The experimental method that follows describes the apparatus that was used to measure the lumen volume and area. The vessel diameter was not measured because the lumen cross-sectional shape is permitted to alter shape during collapse. Thus a simple circular cross section was not assumed for the diameter to be useful. It was chosen to measure lumen area in response to pressure. Alternatively, a controlled fluid volume can be directly injected into the vessel via an infusion pump. The apparatus also allows the study of P-A dynamics by replacing the manual pressure pump with a pulsatile pressure source (9). Dynamics were not studied in this paper. All measurements were performed slowly so as to obtain static P-A data.

The method employed was to use a fluid-filled chamber to contain the vessel (7). Before the vessel was placed in the chamber, its resting wall thickness, length, and diameter were measured by means of a micrometer. The vessel was placed into the chamber and held at each end by a rigid cannula in such a way as to restore its in vivo length (Fig. 3). The chamber was filled with physiological saline at 25°C that was not degassed, allowing a small amount of air at the top. The chamber was then sealed by placing an airtight cover on top. The volume of the vessel was measured with the use of the gas law. That is, because PV equals a constant, pressure is inversely related to the volume of air in the chamber. Thus because the air volume of the chamber can change only due to the vessel volume, the pressure in the chamber must respond in accordance with the gas law. The chamber pressure was then measured by means of a pressure transducer (Motorola MPX50). An external fluid-filled syringe (0.25 ml) was also connected to the chamber to provide a calibrated source of volume change. Chamber pressure change was then calibrated in terms of a syringe volume change of 0.25 ml. To simplify the measurements and maintain linearity, the volume of air in the chamber was chosen such that the total volume change of the vessel resulted in a chamber pressure deviation of, at most, 5 mmHg. In this way, the chamber pressure changes were slight so as to not alter the external vessel pressure significantly. For the precision of the pressure transducer chosen, it was possible to measure volume to within ±2% of the full volume range for the given vessel under study, relying on the syringe as the source of volume calibration. This level of accuracy could be improved by decreasing the volume of air in the chamber at the sacrifice of having larger changes in external pressure and increased nonlinearity of the measurement.

Once the chamber pressure was calibrated to measure vessel volume, the transmural pressure of the vessel was
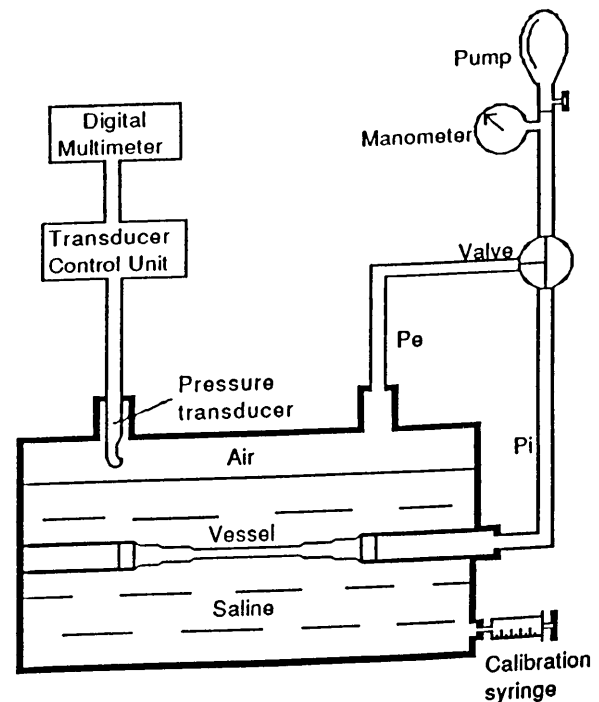

Fig. 3. Apparatus employed to measure P-A curves for all vessels studied. A valve permits separate control of internal (P_i) and external (P_e) vessel pressures. Physiological saline surrounds and fills vessel. A pressure transducer is used to monitor air pressure change and is recalibrated to measure vessel volume.

altered by varying its internal pressure. This was performed by means of the cannulas that were used to extend and hold the vessel in the chamber. One cannula was plugged while the opposite one was connected to a pressure pump and manometer. Before the cannula was plugged, the vessel was filled with saline.

Vessel volume was measured as a function of transmural pressure over the range of −100 to 150 mmHg. In each case, the vessel was cycled up and down over the entire range of pressures until a stable P-A curve was obtained. The data provided were for three cycles of increasing and decreasing transmural pressure after the stabilizing cycles. The vessel volume was converted to area by dividing by the vessel length, assuming that the lumen area is approximately uniform over the vessel length. Six measurements of lumen area were obtained at fixed changes in transmural pressure. The minimum number of pressure measurements was 20, at approximately equal intervals of pressure and equal sample interval of 30 s. The data shown in all figures are the mean lumen area for each level of pressure. Error bars are not shown for any of the data because the standard deviations were found to be <2% of the mean values for all vessels studied. It should be noted that the sampling procedure described here was found to be important in attaining such a high degree of reproducibility of the data so that time-dependent effects, such as hysteresis, are minimized. Also, the level of smooth muscle activity was not determined. But, due to the high reproducibility of our data, it can be assumed to be in a constant state during the course of the measurements.

Model Evaluation

The set of constants was determined for the models of *Eqs. 9* and *17* for each specific vessel by means of nonlinear regression to the P-A data with a Marquardt-Levenberg algorithm (24). Convergence was established when the mean squared error of the residuals changes <0.01% between iterations. Presumably, a minimum in error is achieved for the parameter values that correspond to this point. The initial parameter values employed were within the expected range of values (20%), and the parameters were found to converge to consistent values. This was investigated by varying the initial values of each parameter before regression. In our experience, it was necessary to employ at least 20 points uniformly distributed over the full range of pressure. It is likely that higher standard deviations than those obtained in these experiments may require more data points to obtain convergence. The statistics and plotting were carried out through the use of the graphic software SigmaPlot (Jandel Scientific) on an Apple Macintosh IIvx computer. The parameters found from the nonlinear regression were inserted into the model and were used to compute the transmural pressure corresponding to each measured value of lumen area. The model-derived pressures were then compared with the actual P-A data by evaluating the mean error of estimate. In all cases, the compliance curves were computed from the derivative of area with respect to pressure. Derivatives were computed numerically with the forward difference method.

Arterial Hypertrophy Model

Studies were performed with the geometric model to investigate the alterations in the P-A curve during vascular hypertrophy for two different patterns of growth. The P-A curve of the canine carotid artery, a medium-sized artery, was selected to represent the control conditions (normal vessel).

In each hypertrophy modeled, the wall material properties were assumed to be unchanged. In terms of the model, this means that the parameters a' and b' were held constant in *Eq. 13* at the values obtained for the normal carotid artery. This also assumes that smooth muscle activation remains constant. Some evidence for an invariant wall material property can be found from an animal study on hypertension (4). Hence only geometric effects were being analyzed in this study.

In the first case studied, vascular hypertrophy was created by adding wall tissue in the outward direction only. Total tissue volume and wall thickness were increased above the normal vessel size, and the vessel is assumed to hypertrophy by growth. This was accomplished by increasing the value of h_b in the model. The second kind of hypertrophy modeled was remodeling. In this case, wall thickness was increased while the wall cross-sectional area or volume per unit length was maintained constant. Given a fixed A_w and the prescribed h_b, it was necessary to find the decrease in lumen area due to increased wall thickness from

$$r_{\mathrm{b}} = \left[\frac{A_{\mathrm{w}}}{\pi \gamma (\gamma + 2.0)} \right]^{1/2} \qquad (21)$$

where

$$\gamma = \frac{h_{\mathrm{bc}}}{r_{\mathrm{bc}}} \qquad (22)$$

The wall thickness of the carotid and femoral arteries has been observed to increase in a range of up to 100% above normal and by an average of 23% in hypertensive humans (14). In the late stages of the disease, a doubling of wall thickness can be found. Thus the wall thickness was varied in the model from normal to +100% above the control value in increments of 25%. A family of P-A curves and their corresponding compliance curves were generated for each value of wall thickness and for both patterns of hypertrophy.

RESULTS

Both models were found to apply well to each vessel type studied here. A worst-case (Tygon tube) mean error of estimate in pressure of <10.7 mmHg and a standard deviation of 13.5 mmHg between the lumped model of *Eq. 9* and the data were found, and a mean error of estimate of <7.9 mmHg and standard deviation of 10.1 mmHg for the geometric model of *Eq. 20* were found. But because this vessel is the least compliant, it was measured over a range of 600 mmHg. Taken in this context, the error represents only 1.8% of the range studied. For all vessels studied, the mean error of estimate overall was 3.8 mmHg or 2.5% of the full range measured. Errors were less for blood vessels (see Tables 2 and 3).

Figures 1 and 4–6 show the P-A data for each vessel as well as for the corresponding model results. As can be seen, the two curves on each plot are almost identical over most of the pressure range. Figure 1 shows the results for the canine carotid artery and the corresponding compliance curve plotted as a function of pressure. Figure 4 shows the same curves for the latex elastic vessel. As can be seen, the model performs well for either vascular or elastic vessels. There was virtually no difference between the full geometric model and the lumped model. This was expected because the form of the equations is identical, with the exception that the geometric parameters are expressed in terms of vessel size and wall material properties.
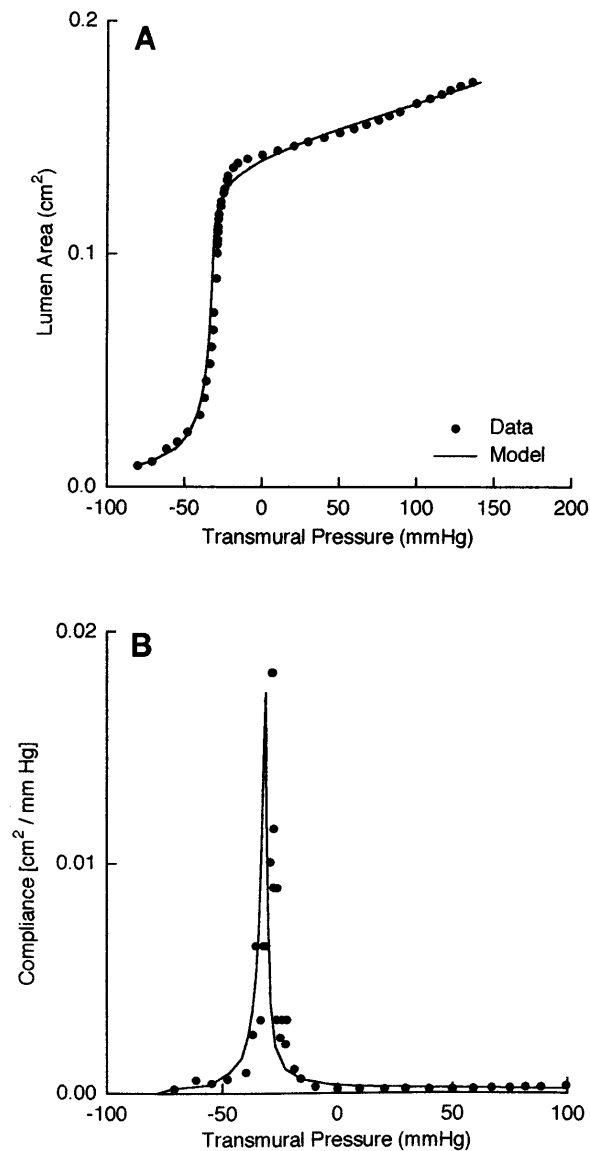
the results of the model developed here can be compared with others, the elastic modulus was evaluated at the point on the stress-strain curve that corresponds with a blood pressure of 100 mmHg. These values were obtained for each vessel and are presented in Table 3. Because the 100-mmHg value for the vein was found to be higher than that for the arteries, its value was redetermined at 10 mmHg, closer to venous pressure. It was then found to be 0.47×10^6 dyn/cm^2, lower than the arterial wall elasticity.

The effects of hypertrophy on the P-A curve can be seen in Fig. 7. A crossover point is observable, i.e., a point of intersection of the P-A hypertrophy curve with its nonhypertrophied P-A curve. The pressure range from negative to low values, as seen in Fig. 7B, displays a leftward shift in the P-A curve. That is, at any given pressure, the lumen area decreases with an increase in hypertrophy. The high-pressure region behaves in just the reverse way: at any given pressure, the lumen area
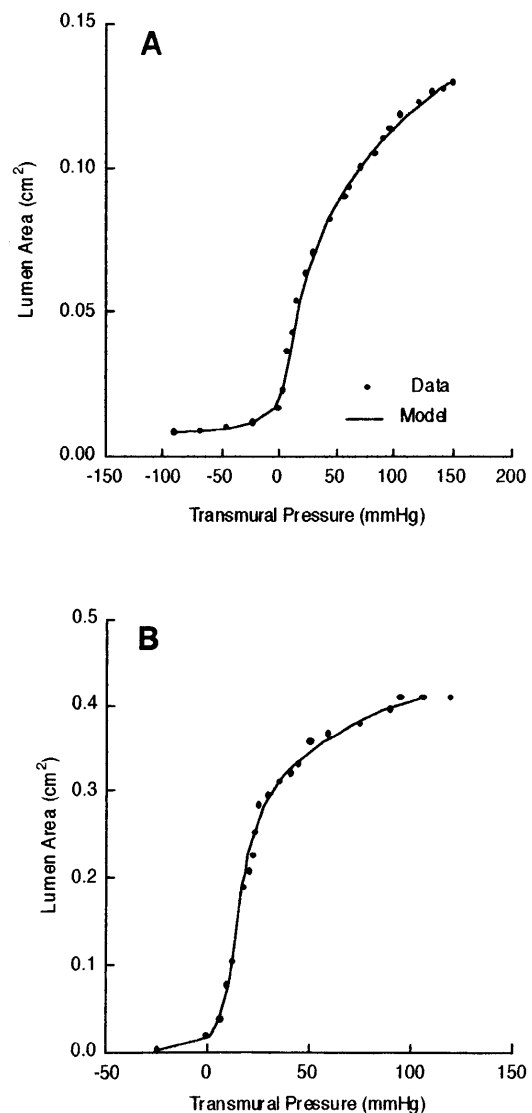

Fig. 4. *A*: latex vessel P-A data and corresponding geometric model-derived relationships. *B*: compliance-pressure curve for model and data in *A*.

Table 1 provides the measured characteristics of each vessel studied. Table 2 provides, for the lumped model, the modeling parameters and constants, and a measure of the quality of the model fit to the data (the mean absolute estimate error). Table 3 provides the results for the parameters and constants of the geometric model and the mean absolute error for each vessel studied.

The regions of collapse and distension each require the parameters E, a', and b' that determine the stress-strain curve of the vessel wall material. The constant E represents the wall elastic modulus during collapse. It was assumed that the value of wall elasticity is relatively constant during collapse because the perimeter of the vessel is not stretched. During wall stretch, though, the value of E becomes a function of stretch and must be determined from the slope of the stress-strain curve. Most studies of wall elasticity measure this value at the operating range of blood pressure. So that

Fig. 5. Blood vessel P-A data and corresponding geometric model-derived relationships for a canine femoral artery (*A*) and canine jugular vein (*B*).
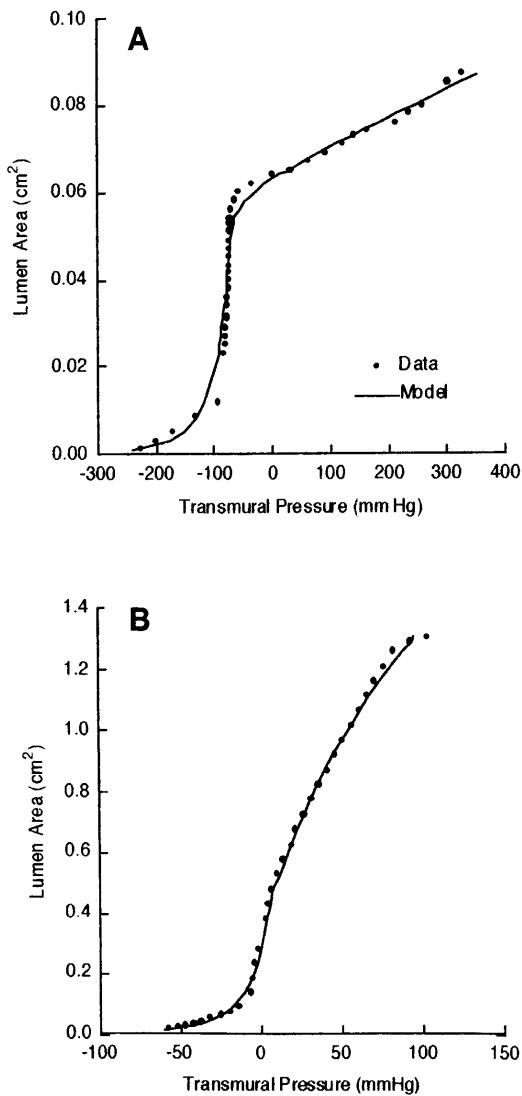
Fig. 6. Model and data for P-A curves for Tygon tubing (*A*) and Penrose drainage tubing (*B*).

increases with hypertrophy. Thus there was a rightward shift in the P-A curve in this region.

Figure 8 shows the corresponding compliance curves of the modeled results of Fig. 7. This family of curves shows three interesting features. For pressures higher than ~15 mmHg, the compliance curve shifts up at any given pressure. Thus compliance increases with hyper-

Table 1. *Vessel measured characteristics*

Vessel Type	A_0, cm^2	A_b, cm^2	P_b, mmHg	h_b, cm
Canine femoral artery	0.0603	0.0600	0.00	0.0660
Canine carotid artery	0.0164	0.0361	7.50	0.0787
Canine jugular vein	0.0189	0.1040	12.0	0.0401
Penrose tube	0.3160	0.4310	4.54	0.0445
Latex tube	0.1423	0.1110	−28.4	0.0381
Tygon tube	0.0640	0.0450	−73.0	0.0382

Values are averages of 6 trials for each vessel. A_0, lumen cross-sectional area at 0 transmural pressure; A_b, lumen cross-sectional area at maximum compliance point (MCP); P_b, buckling pressure (transmural pressure at MCP); h_b, vessel wall thickness at MCP.

trophy. The final behavior observed was a decrease in compliance at any given pressure for the collapse region, seen on the plot as a downward shift in the compliance curve.

Pure arterial wall remodeling resulted in a lumen area that was found to decrease for any increase in wall thickness (Fig. 9). The compliance curves that correspond to remodeling demonstrate the greatest reductions in the low and negative range of pressures (Fig. 10). In particular, it is interesting to note that C_{max} alters to a much greater extent than for hypertrophy with growth. Alternatively, the changes in compliance are small in the normal and hypertensive ranges of blood pressure compared with growth.

Parameter Sensitivity

Because wall material property values were not available for the growth model, it was necessary to examine the effect of their variation. The sensitivity to each parameter was examined as well. Parameter sensitivity was determined only for the values that were computed to best fit the femoral artery data. A fractional change, <1% of each parameter value, was applied to compute the corresponding change in transmural pressure. Sensitivity was then reported as the fractional change in transmural pressure normalized by the fractional change in the parameter (Fig. 11).

The parameter sensitivity results were different in the distension and collapse ranges. For example, the parameters *n* and *E* have effects during collapse but no effects during distension. This was expected because the model equations require that these parameters control the collapse pressure term P_c. Similarly, the parameters *a'* and *b'* were found to alter only the distension range of pressure. Thus the extreme distension and collapse regions of the P-A curve may be modeled separately, if desired. This approach fails, though, near the buckling pressure and area where all parameters are necessary. For blood vessels, the complete model was necessary for the range ± 15 mmHg. The other parameters common to the distension and collapse terms were found to be effective in their corresponding ranges.

To further examine the effect of the wall material parameters *a'* and *b'* on the hypertrophy predictions, the positive range of pressure was computed for a ±10% change in each parameter. This computation was performed for the condition of outward wall growth (Fig. 12). The wall thickness was doubled in comparison with the control values. It was found that increasing either *a'* or *b'* reduces the lumen area at a given positive pressure. Decreasing *a'* or *b'* resulted in the opposite response.

DISCUSSION

Vessel Model

The vessel P-A model was provided here in two forms: a lumped P-A model and a geometric P-A model. Depending on the application or study, the lumped P-A model may be employed, for example, if it is necessary

Table 2. *Basic model parameters*

Vessel Type	A_0, cm^2	A_b, cm^2	P_b, mmHg	a, mmHg	b, unitless	$\widehat{EI}$, mmHg	n, unitless	Mean Deviation, mmHg
Canine femoral artery	0.0545	0.0583	−1.26	13.4	1.39	11.7	0.548	3.25
Canine carotid artery	0.0200	0.0189	−0.640	11.9	0.438	4.14	3.76	2.43
Canine jugular vein	0.0197	0.0738	10.1	0.327	1.23	35.5	0.187	2.66
Penrose tube	0.286	0.455	5.39	40.4	0.588	27.8	0.385	1.86
Latex tube	0.141	0.137	−29.9	5,197.0	0.123	3.14	1.05	3.80
Tygon tube	0.0630	0.0592	−67.8	12,980	0.0660	92.3	0.283	10.7

Values were determined with lumped pressure-area (P-A) model for each vessel. *a*, Constant of proportionality termed elastance scale modulus; *b*, exponential rate constant termed elastance scale modulus; $\widehat{EI}$, contant of proportionality termed flexural rigidity; *n*, constant defining degree of curvature of P-A hyperbola.

only to model data. If dimensional or wall vascular properties are of interest, then the geometric model is more appropriate. It was shown here that either form of the P-A model can model blood vessel and latex tube data equally well over the full range of blood pressures including vessel collapse. For all vessels studied, the mean absolute error between the model and the data was <11 mmHg. In the case of blood vessels, this error was <3.5 mmHg for both models. Thus the performance of both models was indistinguishable in terms of error. The only functional difference between the models accounts for wall thickness changes with lumen area. But because the distension relationship for both models incorporates an exponential, the presence of the wall thickness variable can be accounted for by altering the exponential parameter.

The models fit the vascular vessel P-A data somewhat better than those for the elastic vessels. This is because the blood vessels more closely approximate the exponential stress-strain behavior expressed during distension. That is, the wall elastic properties are nonlinear, giving rise to an exponential P-A curve for positive pressures. By contrast, latex vessels possess a more linear elastic material property. It was found that the series approximation form of the exponential stress-to-stretch ratio is superior in representing the elastic vessels (results not provided here). When performing a fit, the strain-squared term is typically forced to become small. This leaves the linear term present, resulting in better accuracy. The exponential form was retained here because it always provided the lowest error for blood vessels, which is the main focus. The Penrose tubing P-A relationship differs in this respect, though, by more closely matching the model than the other

elastic tubes. This could be explained by its natural tendency to partially collapse at zero pressure.

Although the parameters a' and b' were used in this study to specify the shape of the stress-strain curve, researchers (5) have employed the incremental wall elastic modulus as a measure of wall stiffness. This is found from the slope of the stress-strain curve. Because the stress curve is nonlinear, the elastic modulus is not a constant and varies with blood pressure. Thus most studies refer the elastic modulus to a specific pressure or lumen area, most commonly, the normal blood pressure range. So that a comparison can be made, the elastic modulus was evaluated from the slope of the model-generated stress-strain curve at a point corresponding to 100 mmHg. These values corresponded well with those reported for the dog in other studies (13).

Hypertrophy

The P-A model was developed to study the vascular hypertrophy that occurs with hypertension, as well as for other hemodynamic applications. It has been suggested earlier that the vascular wall thickens to reduce wall stress and protect the vascular tissue from elevated luminal pressures. In fact, in any type of hypertension, wall thickening of the medial layer is always observed (21). Other researchers suggested that continual hypertrophy leads to lumen narrowing because of wall thickening. This increases blood flow resistance and further increases blood pressure, i.e., the structural theory of hypertension (12). Differing theories consider vascular hypertrophy as either the cause of hypertension or the secondary response to it.

Table 3. *Geometric model parameters*

Vessel Type	A_0, cm^2	A_b, cm^2	P_b, mmHg	a', mmHg	b', unitless	E, mmHg	n, unitless	E at 100 mmHg, dyn/cm^2	Mean Deviation, mmHg
Canine femoral artery	0.0592	0.0604	−0.928	21.3	8.04	1,840	0.54	3.9×10^6	1.98
Canine carotid artery	0.0177	0.0409	−7.90	24.5	6.54	29.2	3.38	5.2×10^6	2.15
Canine jugular vein	0.0209	0.152	15.6	3.20	10.7	9,530	0.137	17.0×10^6	2.68
Penrose tube	0.286	0.0478	6.07	158	4.31	$1.98e^5$	0.383	1.6×10^6	1.78
Latex tube	0.139	0.142	−31.2	23,400	0.577	4,440	1.16	18.6×10^6	4.04
Tygon tube	0.0635	0.0613	−65.6	30,900	0.444	64,500	0.246	18.7×10^6	7.90

Values were determined with geometric P-A model for each vessel. *a′*, constant of proportionality termed wall elastic scale modulus; *b′*, exponential rate constant termed wall elastic scale modulus; *E*, wall elastic modulus (elasticity).
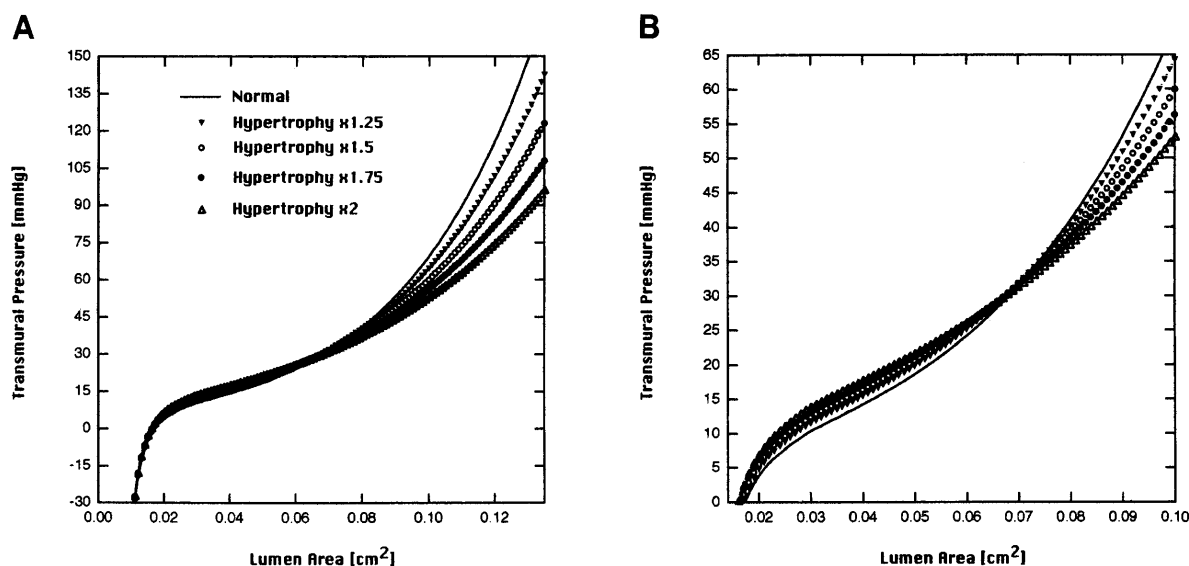
Fig. 7. Results of arterial hypertrophy model for a canine carotid artery. *A*: full range of P-A relationships. *B*: stretch region magnified to show a crossover point. Wall thickness was increased with growth of wall cross section. Five degrees of hypertrophy (change in wall thickness) are shown: 0 (normal), 25 (×1.25), 50 (×1.50), 75 (×1.75), and 100% (×2).

The pattern of wall thickening for vascular hypertrophy is of interest to researchers. In particular, the question arises, What is the effect of wall hypertrophy on lumen size and vessel compliance over the complete range of pressures? Heagerty et al. (17) found that peripheral arteries, small arteries, and arterioles typically remodel with hypertension. Thus wall thickness increases and the wall thickness-to-diameter ratio increases, whereas the wall cross-sectional area is found to remain nearly constant. This constraint was applied to the P-A model and was used to find lumen pressure and compliance versus blood pressure (Figs. 9 and 10). The model results show a decrease in lumen diameter

of 9.5% for a wall thickening of 25% compared with control values at a transmural pressure of 100 mmHg. This is consistent with the observations of Heagerty et al., who found that lumen diameter decreases 13% for a 17% increase in wall thickness. Although experimental results are available for unpressurized vessels (21), the model indicates that the lumen area should decrease with remodeling for all levels of pressure. Functionally, this may be expected because the reduced lumen size
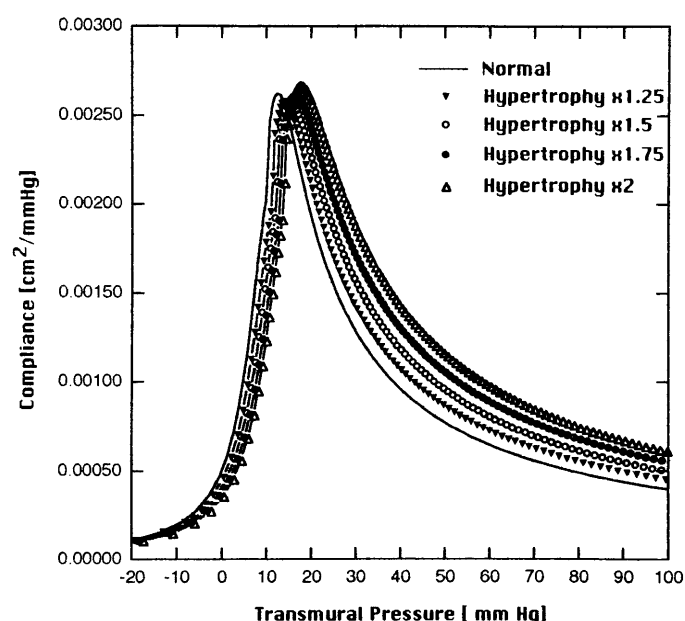

Fig. 8. Compliance-pressure curves for P-A model of hypertrophic artery in Fig. 7.
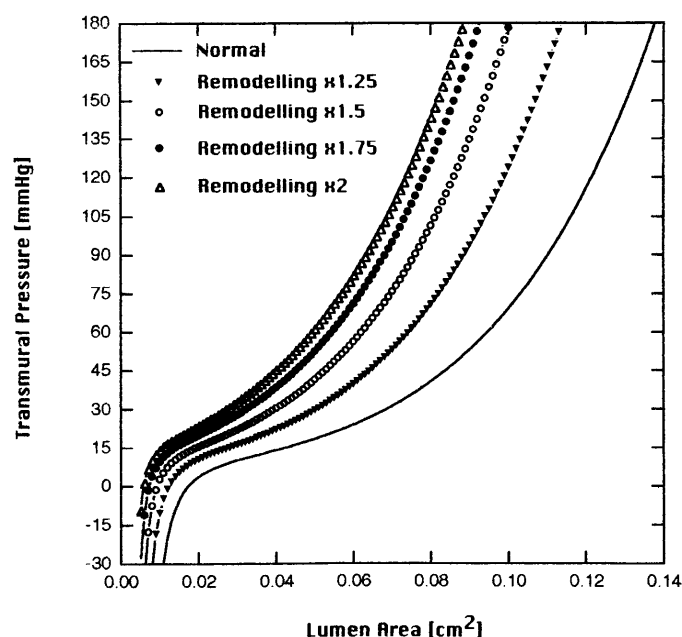

Fig. 9. P-A curves for a canine carotid artery as found from model for remodeling. Wall thickness was increased, but wall cross-sectional area was constant. Five degrees of remodeling (change in wall thickness) are shown: 0% (normal), 25 (×1.25), 50 (×1.50), 75 (×1.75), and 100% (×2).
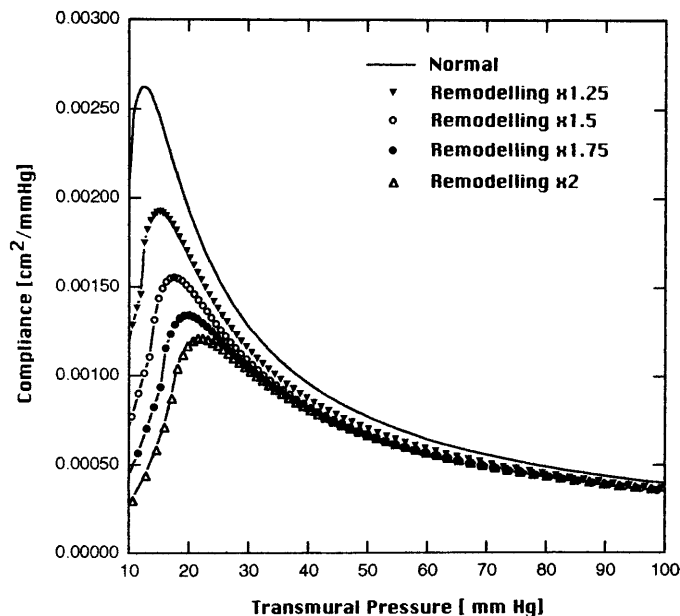
Fig. 10. Compliance-pressure curves for remodeled artery P-A curves in Fig. 9.

will increase flow resistance and protect the distal vascular bed from the elevated pressures.

After remodeling occurs, compliance either decreases, stays constant, or increases depending on the severity of hypertrophy and the elevation of blood pressure. The effect of remodeling and wall thickening on compliance was minimal in the normal- to high-pressure range. Thus the compliance change in remodeled arteries for high pressure is primarily due to pressure dependency and/or wall material changes and not to the wall thickness alteration.

The other pattern of vascular hypertrophy modeled was outward wall growth due to wall thickening. But, unlike that for remodeling, the wall area increases. The lumen-narrowing response of this pattern of hypertrophy was similar to that of remodeling for low pressures but caused an increase in lumen size for normal to high pressures (Fig. 7). This, at first, was seemingly a contradiction. But, recently, Hayoz et al. (16) provided supporting data. When examining the lumen size in normotensive and hypertensive subjects at the same pressure, these researchers reported a 1% increase in the radial arterial diameter. This corresponds with the model prediction of a +1.6% change in lumen diameter for the +25% wall-thickening curve at a transmural pressure of 100 mmHg. The growth pattern is thus dependent on the anatomic location of the vessel. These researchers performed their studies on medium to large arteries. Because these vessels primarily serve as conduits for blood flow, it may be beneficial for them to hypertrophy such that wall stresses are reduced yet flow resistance is maintained or slightly diminished.

Although the effect of geometry and wall growth of the vessel is emphasized here, it should be clear that wall material properties are not excluded from the changes that occur in the wall of a hypertrophied vessel. For example, it was shown that lumen area

would also increase for a reduction in wall stiffness (Fig. 12). But wall stiffness is generally observed to increase in hypertensive and elderly patients. Despite this, the model predicts that a 10% increase in wall stiffness can still lead to an increasing lumen area at high pressure in hypertrophied vessels. Because a decrease in wall stiffness is not likely in disease conditions, it may be that wall thickening is a more probable explanation for the observed effects.

It should be noted, though, that hypertrophy with growth leads to a lumen area decrease for low positive pressures (Fig. 7). Thus it would seem that lumen narrowing with hypertrophy is consistent throughout
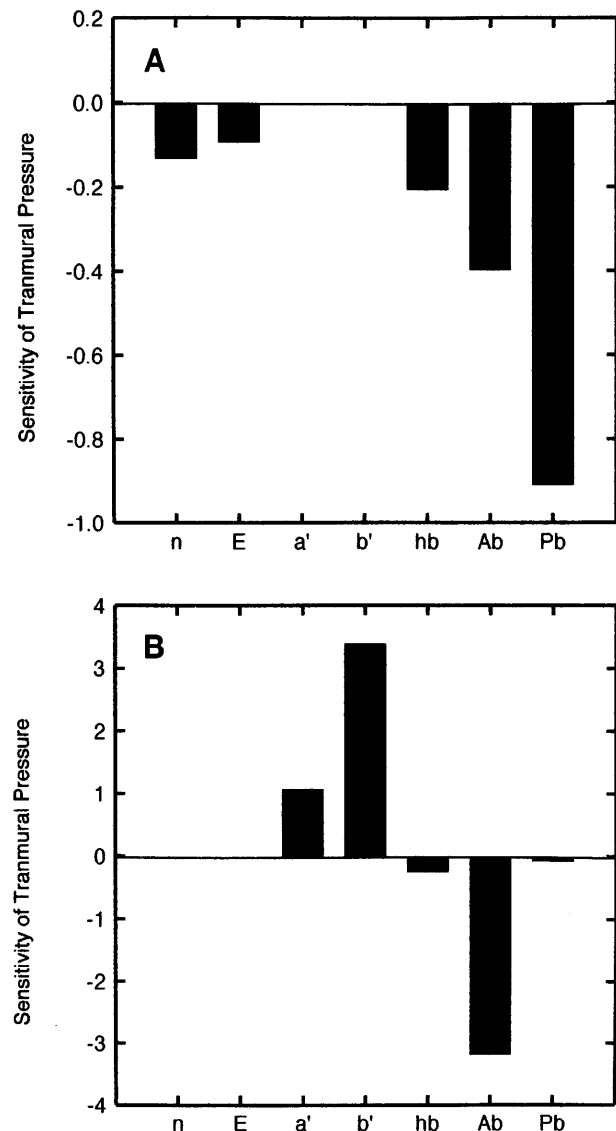

Fig. 11. Sensitivity of transmural pressure to variation in each model parameter during vessel collapse (A) and vessel distension (B). Sensitivity was computed as fractional change in transmural pressure normalized by fractional change in the given parameter. n, Constant defining degree of curvature of hyperbolic P-A relationship; E, wall elastic modulus (elasticity); a', constant of proportionality termed wall elastic scale modulus; b', exponential rate constant termed wall elastic rate modulus; h_b, vessel wall thickness at maximum compliance point.
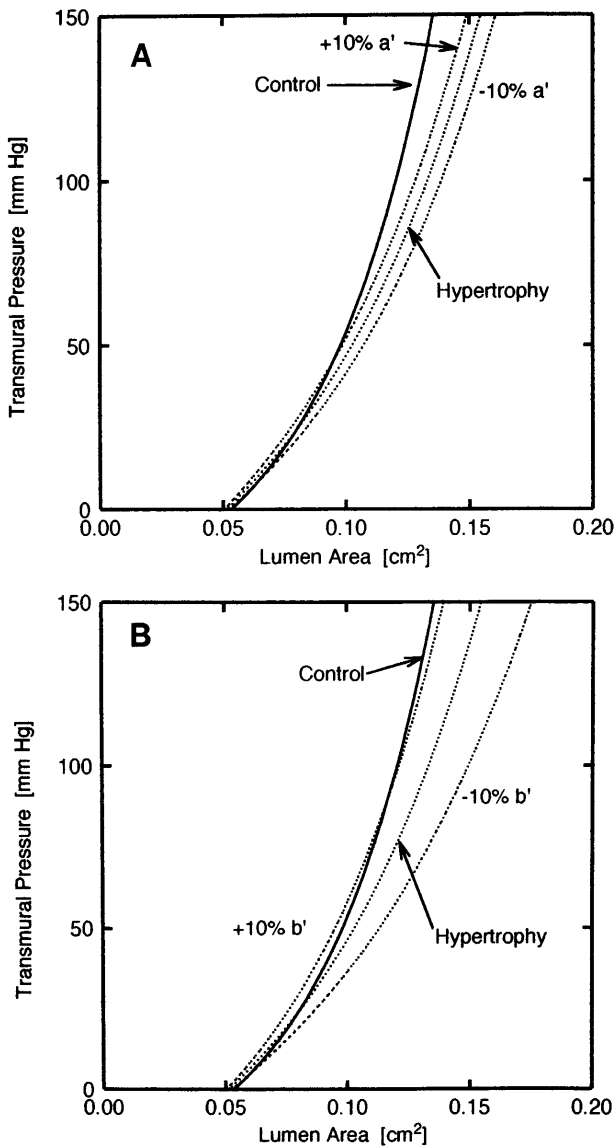
Fig. 12. Control P-A curves computed from model with carotid artery parameters. For each hypertrophy curve, wall material parameters a' (*A*) and b' (*B*) were varied ±10% around control values. Hypertrophy curves were computed for a doubling of wall thickness in an outward growth pattern.

the systemic arterial tree when vessels from experimental animals at low positive pressure are examined. The discrepancy of lumen size increase arises only when hypertrophied vessels are compared with nonhypertrophied vessels at high pressures.

Two regions of behavior were seen with hypertrophy, i.e., regions of increasing and decreasing lumen area with wall thickness. This appears as a crossover point in Fig. 7. For small muscular arteries and arterioles, only a reduced lumen area with hypertrophy has been reported. These arteries might display both regions of behavior but because of their low wall thickness or high wall thickness-to-lumen radius ratio, the crossover point might be at a much higher pressure than is physiological, making its existence for these vessels unlikely. The opposite can be said for medium to large

muscular arteries because of their thick walls and smaller wall thickness-to-lumen radius ratios. These arteries show an increase in lumen area with hypertrophy at high pressures (4) and a decrease at lower pressures. The crossover point of the P-A curve is typically not reported by others. This might be because the pressure range that is usually investigated is often incomplete. Furthermore, observations of the full P-A curve would be necessary before and after hypertrophy takes place. Such complete experimental studies are lacking in the literature. Weizsacker et al. (29), though, did report the presence of crossover in longitudinal force-length curves for differing pressures in nonhypertrophied vessels.

Last, the arterial compliance changes due to hypertrophy with growth were modeled (Fig. 8). The change in compliance due to this type of growth pattern was inverse to that of remodeling and shows a much larger increase in compliance over the normal-to-hypertensive pressure range. Hayoz et al. (16) also observed this from human radial artery data. This group described the compliance curve changes as an upward "resetting" of compliance by 25% for the hypertensive patients. This corresponded well with the compliance curve for the 25% increase in wall thickness of the model. Thus normal large arteries and those that have hypertrophied are found to have nearly equal compliance when the compliance is determined at the subject's resting pressure. This pattern of growth may be important for large arteries such that the pulse pressure is maintained or not excessively increased (2).

There would appear to be a discrepancy between the lumen area and compliance change due to hypertrophy with growth compared with that of remodeling. It is generally assumed that a vessel's compliance should decrease with increased wall thickness, as in remodeling. The results shown here demonstrate that the pattern of wall thickening is important to determine this outcome. Thus the opposite response of compliance for hypertrophy can be explained as follows. If the wall growth is outward while lumen area is maintained, the vessel wall stress must be reduced according to Laplace's law. Reduced wall stress, in turn, reduces wall stiffness, making the vessel more compliant and also able to increase lumen size more readily. In the case of remodeling, the same situation is true with the exception that there is some inward wall growth. This decreases the lumen area more rapidly than the wall stress and stiffness.

A simple test was performed to examine the above concepts. Consider, for example, the case where hypertrophy occurs while the wall material elastic modulus is a constant. That is, assume that the vessel wall consists of a linear elastic material. This situation is nearly true for the latex vessels that were studied here. Thus, by employing a linear elastic wall material and analyzing an outward wall growth, as for the blood vessel, it was found that lumen area and compliance decrease at high pressures compared with the nonhypertrophied wall. This was opposite to what was found for the outward hypertrophied artery. Hence the fact that

wall stiffness and wall stress decrease due to wall thickening permits the artery to achieve increased lumen area and compliance. The nonlinear elastic wall property is crucial for this outcome.

The modeling case of hypertrophy with outward wall growth was intriguing because it does explain why lumen area and compliance are increased. It was interesting to reexamine these results in the event that elastic stiffness increases. It was then found that the lumen area and compliance were returned toward control values. Thus it appears that the outward wall-thickening result may only be observed with the provision that wall stiffness is not increased much above normal levels. Unfortunately, in vivo studies have not been performed as yet to investigate this possibility. The alternative explanation that wall stiffness decreases during hypertrophy is not typically observed in hypertension.

It should be clear that the model presented here, although corresponding closely to our data and those reported by others (1, 14, 16, 17), focuses on the effect of wall growth pattern. In an actual disease process, it may be expected that other parameters can change as well. For example, it was assumed that the wall material properties are invariant after hypertrophy. The geometric parameter A_b and the collapse parameters were invariant as well. Finally, the roles of residual wall stress and longitudinal tether were not considered. These parameters may likely change with a pathology and need to be fully evaluated in future experimental studies. The fact that other parameters may vary in hypertension may be a limitation of this modeling approach.

In addition to being able to model normal passive, physiologically active, and pathological effects on the P-A curve, the model can also be easily modified to account for the effects of tether (29). These are the effects due to longitudinal stress on a vessel resulting from an application of an axial force. This can be achieved by merely changing h_b and A_b. For increased longitudinal stress, h_b and A_b are decreased. In this study, longitudinal stress was assumed to be constant at in vivo levels.

The role of residual wall stress was not studied explicitly in this paper. Residual stress can be defined as the existence of a stress distribution across the vessel wall even when transmural pressure is zero. This stress distribution results in a bending stress that would cause the vessel to open if it were cut longitudinally. The model measures this bending stress by means of the P_c term. Hence residual stress is implicit in the value of P_c where it is negative. At zero transmural pressure, this term was balanced by the contribution of wall stress due to the stretch term P_s. In the example of Fig. 2, P_c was shown as a decomposition of the total transmural pressure. It can be seen that P_c is nonzero even at zero transmural pressure. Hence the presence of residual stress must indirectly result in a collapse pressure, although its transmural distribution cannot be resolved by this model. Because the parameters in this term were not varied with hypertrophy, it

may be assumed that residual stress is invariant in the model predictions.

Because the P-A data curves were obtained from averages of the periodically cycled lumen volume and pressure, the viscous dynamic effects were removed. This is thus a static model of a P-A curve of a vessel. Because hypertrophy, though, is a chronic, long-term process, the results and discussion provided in this regard are not affected by viscosity.

In conclusion, the present study overcomes the problem of modeling the P-A curve of vessels for the complete range of pressure by combining two regions of behavior, collapse and distension, into a single model of a vascular segment. This was found to be critical for low blood pressure levels where the two regions overlap, allowing for more realistic applications involving the pressure and flow dynamics in blood vessels. Moreover, the model allows the variation in vessel size that earlier empirical models could not, thus permitting the study of vascular hypertrophy performed here. The model was validated here in comparison with different types of blood vessels and elastic tubing, where model errors were found to be commensurate with the level of experimental error.

Two patterns of arterial wall thickening were studied with the vessel model. The first pattern was hypertrophy with outward wall growth. This pattern of growth was found to produce increased arterial compliance and lumen size for hypertensive pressure. In addition, it was found that outward hypertrophy led to increased lumen size only for normal to high blood pressure. Otherwise, at low pressures, lumen narrowing was found to occur. The second pattern was wall thickening with remodeling (no wall growth). This produced the widely observed decrease in compliance as well as in lumen area. It was concluded that the wall growth pattern is an important determinant of vascular compliance and lumen size change with wall thickness.

REFERENCES

1. **Armentano, R., A. Simon, J. Levenson, N. P. Chaw, J. L. Megnien, and R. Pickel.** Mechanical pressure versus intrinsic effects of hypertension on large arteries in humans. *Hypertension* 18: 657–664, 1991.
2. **Berger, D., and J. J.-K. Li.** Concurrent compliance reduction and increased peripheral resistance in the manifestation of isolated systolic hypertension. *Am. J. Cardiol.* 65: 67–71, 1990.
3. **Beyar, R., R. Caminker, D. Manor, and S. Sideman.** Coronary flow patterns in normal and ischemic hearts: transmyocardial and artery to vein distribution. *Ann. Biomed. Eng.* 21: 435–458, 1991.
4. **Brayden, J. E., W. Halpern, and L. R. Brann.** Biochemical and mechanical properties of resistance arteries from normotensive and hypertensive rats. *Hypertension* 5: 17–25, 1983.
5. **Cox, R. H.** Mechanical properties of arteries in hypertension. In: *Blood Vessel Changes in Hypertension: Structure and Function,* edited by R. M. K. W. Lee. Boca Raton, FL: CRC, 1989, chapt. 4, p. 65–98.
6. **Drzewiecki, G. M., J. Melbin, and A. Noordergraaf.** The Korotkoff sound. *Ann. Biomed. Eng.* 17: 325–359, 1989.

7. **Drzewiecki, G. M., and I. Moubarak.** Transmural pressure-area relation for veins and arteries. *Proc. Annu. Northeast Bioeng. Conf. 14th Durham NH 1988,* p. 269–272.

8. **Drzewiecki, G. M., S. Y. Rabbany, J. Melbin, and A. Noordergraaf.** Generalization of the transmural pressure-area relation for the femoral artery. *Proc. Annu. Conf. IEEE/EMBS 7th Chicago IL 1985,* p. 507–510.

9. **Field, S., and G. Drzewiecki.** Linear hydraulic pressure-pulse actuator (LHPA): a versatile instrument that produces a simulated blood pressure pulse wave for small sized vessels. *IEEE Trans. Biomed. Eng.* 43: 663–668, 1996.

10. **Field, S., C. Horton, G. Drzewiecki, and J. K.-J. Li.** General pressure-area relationship for collapsible vessels and elastic tubing. *Proc. Soc. Biomed. Eng. Conf. 13th Washington DC 1994,* p. 1011–1014.

11. **Flaherty, J. E., J. B. Keller, and S. I. Rubinow.** Post buckling behavior of elastic tubes and rings with opposite sides in contact. *J. Appl. Math.* 23: 446–455, 1972.

12. **Folkow, B.** Physiological aspects of primary hypertension. *Physiol. Rev.* 62: 347–504, 1982.

13. **Fung, Y. C.** *Biodynamics: Circulation.* New York: Springer-Verlag, 1984.

14. **Gariepy, J., M. Massonneau, J. Levenson, D. Heudes, A. Simon, and the Groupe de Prevention Cardio-Vasculaire en Medecine du Travail.** Evidence for in vivo carotid and femoral wall thickening in human hypertension. *Hypertension* 22: 111–118, 1993.

15. **Glantz, S.** A constitutive relation for the passive properties of muscle. *J. Biomech.* 17: 137–145, 1974.

16. **Hayoz, D., B. Rutschmann, F. Perret, M. Niederberger, Y. Tardy, V. Mooser, J. Nussberger, B. Waesber, and H. R. Brunner.** Conduit artery compliance and distensibility are not necessarily reduced in hypertension. *Hypertension* 20: 1–6, 1992.

17. **Heagerty, A. M., C. Aalkjaer, S. J. Band, N. Korsgaard, and M. J. Mulvany.** Small artery structure in hypertension—dual processes of remodelling and growth. *Hypertension* 21: 391–397, 1993.

18. **Kresch, E., and A. Noordergraaf.** Cross-sectional shape of collapsible tubes. *Biophys. J.* 12: 274–294, 1972.

19. **Li, J. K.-J., T. Cui, and G. M. Drzewiecki.** A nonlinear model of the arterial system incorporating a pressure-dependent compliance. *IEEE Trans. Biomed. Eng.* 37: 673–678, 1990.

20. **Moreno, A. H., A. I. Katz, and L. D. Gold.** An integrated approach to the study of the venous system with steps toward a detailed model of the dynamics of venous return to the right heart. *IEEE Trans. Biomed. Eng.* 16: 308–324, 1969.

21. **Mulvany, M. J.** Are vascular abnormalities a primary cause or secondary consequence of hypertension? *Hypertension* 18: I-52–I-57, 1991.

22. **Noordergraaf, A.** *Circulatory System Dynamics.* New York: Academic, 1978.

23. **Palladino, J., G. Drzewiecki, and A. Noordergraaf.** Modelling strategies in physiology. In: *The Biomedical Engineering Handbook,* edited by J. Bronzino. Boca Raton, FL: CRC, 1995, p. 2367–2374.

24. **Press, W. H., B. P. Flannery, S. A. Teukolsky, and W. T. Vetterling.** *Numerical Recipes.* Cambridge, UK: Cambridge Univ. Press, 1986.

25. **Shapiro, A. H.** Steady flow in collapsible tubes. *J. Biomech. Eng.* 99: 126–147, 1977.

26. **Sipkema, P., and N. Westerhof.** Mechanics of a thin walled collapsible micro-tube. *Ann. Biomed. Eng.* 17: 203–217, 1989.

27. **Von Mises, R.** Der kritische aussendruck zylindrischer Rohre. *Verh. Dtsch. Ing. Z.* 58: 750–755, 1914.

28. **Walker-Caprioglio, H. M., J. A. Trotter, S. A. Little, and L. J. McGuffee.** Organization of cells and extracellular matrix in mesenteric arteries of spontaneously hypertensive rats. *Cell Tissue Res.* 269: 141–149, 1992.

29. **Weizsacker, H. W., H. Lambert, and K. Pascale.** Analysis of the passive mechanical properties of rat carotid arteries. *J. Biomech.* 16: 703–715, 1983.

30. **Westerhof, N., F. Bosman, C. J. De Vries, and A. Noordergraaf.** Analog studies of the human systemic arterial tree. *J. Biomech.* 2: 121–143, 1968.